Ann Surg Oncol (2011) 18:1175–1184
DOI 10.1245/s10434-010-1391-7

Annals of
SURGICAL ONCOLOGY
OFFICIAL JOURNAL OF THE SOCIETY OF SURGICAL ONCOLOGY

ORIGINAL ARTICLE – TRANSLATIONAL RESEARCH AND BIOMARKERS

Hepatic Stellate Cells Accelerate the Malignant Behavior of Cholangiocarcinoma Cells

Hirohisa Okabe, MD[1], Toru Beppu, PhD[1], Hiromitsu Hayashi, PhD[1], Takatoshi Ishiko, PhD[1], Toshiro Masuda, PhD[1], Ryu Otao, MD[1], Hasita Horlad[1], Hirohumi Jono, PhD[2], Mitsuharu Ueda, PhD[2], Satoru Shinriki PhD[2], Yukio Ando, PhD[2], and Hideo Baba, PhD[1]

[1]Department of Gastroenterological Surgery, Graduate School of Medical Sciences, Kumamoto University, Kumamoto, Japan; [2]Department of Diagnostic Medicine, Graduate School of Life Sciences, Kumamoto University, Kumamoto, Japan

ABSTRACT

Background. Although tumor–stromal interaction has been discussed, the role of hepatic stellate (HS) cells against cancer, especially cholangiocarcinoma (CC), has not been clarified. The aim of this study is to investigate the effect of HS cells on CC cell progression in vitro and in vivo.

Methods. The effects of CC conditioned medium (CC-CM) on activation and proliferation of HS cells (LI90 and LX-2), the influences of HS cell CM (HS-CM) on proliferation and invasion of CC cells (HuCCT-1 and RBE), and the effects of their interaction on HUVEC tube formation were assessed using each CM. The effect of HS cells on tumor growth was examined in vivo by subcutaneous co-injection. Cytokine array was performed to assess the secreted proteins induced by their coculture.

Results. CC-CM activated HS cells and increased their proliferation. HS-CM dose-dependently increased CC cell proliferation and invasion. Chemotherapy of CC cells was less effective when treated with HS-CM. HS-CM activated the mitogen-activated protein kinase and Akt pathways in tumor cells. The indirect interaction of CC and HS cells promotes tube formation of human umbilical venous endothelial cells. Subcutaneous co-injection of tumor cells with HS cells in nude mouse resulted in increased tumor size. Several proteins were found in the culture medium induced by their coculture, thought to be key proteins which regulated tumor–stromal interaction.

Conclusions. This study indicates that HS cells play an important role in accelerating cholangiocarcinoma progression and may be a therapeutic target in cholangiocarcinoma.

Intrahepatic cholangiocarcinoma has poor prognosis due to its early lymphatic invasion and distant metastasis.[1–3] Nonmalignant cells in the tumor microenvironment have been reported to play key roles in tumor progression. The tumor microenvironment comprises endothelial cells, pericytes, fibroblasts, and various bone marrow-derived cells (BMDCs) such as macrophages, neutrophils, mast cells, myeloid cell-derived suppressor cells, and mesenchymal stem cells.[4] Among these, cancer-associated fibroblasts (CAFs), the so-called myofibroblasts, are reportedly associated with progression of breast, colon, prostate, and pancreas cancer.[5–8]

Hepatic stellate (HS) cells are activated into myofibroblasts during hepatic fibrogenesis and react to hepatic injury by producing extracellular matrix factors or cytokines, such as transforming growth factor-β (TGF-β), epidermal growth factor (EGF), platelet-derived growth factor (PDGF), and basic fibroblast growth factor (bFGF).[9] Although these factors are important for the cancer microenvironment, the presence and role of HS cells in cancer have not been fully investigated. We have previously suggested that HS cells might be present in liver cancer stroma, and might promote progression of intrahepatic cholangiocarcinoma.[10]

Previous in vitro and in vivo studies on pancreatic cancer have suggested that the interaction of CAFs and cancer cells promotes cancer growth and invasion, and inhibits anti-cancer drug-induced apoptosis.[5,11–13] These

Electronic supplementary material The online version of this article (doi:10.1245/s10434-010-1391-7) contains supplementary material, which is available to authorized users.

First Received: 25 May 2010;
Published Online: 2 November 2010

H. Baba, PhD
e-mail: hdobaba@kumamoto-u.ac.jp

studies revealed that PDGF produced by pancreatic stellate cells enhances growth of pancreatic cancer cells. In addition, cancer cell-activated fibroblasts induced angiogenesis, resulting in production of vascular endothelial growth factor (VEGF).[14,15]

The interaction between HS cells and cholangiocarcinoma cells has not been investigated; therefore, we examined whether HS cells could act as CAFs and accelerate the progression of cholangiocarcinoma cells in vitro and in vivo. Since we wanted to focus on the role of hepatic stellate cells, and cytokines and chemokines from stromal cells have been shown to be of great importance for tumor development, we used a cytokine array and assessed the secreted proteins associated with the tumor–stromal interaction.[16]

MATERIALS AND METHODS

Cell Culture

The HuCCT-1 cell line was obtained from the Cell Resource Center for Biochemical Research, Tohoku University (Sendai, Japan). The RBE cell line and the human HS cell line LI90 were purchased from the Japanese Collection of Research Bioresources (Osaka, Japan).[17] The human HS cell line LX-2 was a kind gift from Scott L. Friedman (Mount Sinai School of Medicine, NY, USA).[18] Tumors were cultured in Roswell Park Memorial Institute (RPMI) medium, and HS cells were cultured in Dulbecco's modified Eagle's medium (DMEM) containing 10% fetal bovine serum (FBS) with penicillin/streptomycin. All cultures were maintained in 5% CO_2 air-humidified atmosphere at 37°C. Human umbilical vein endothelial cells (HUVECs) were purchased from the American Type Culture Collection (VA, USA) and maintained using the EGM-2 bullet kit (Lonza, Basel, Switzerland).

Preparation of Conditioned Media

The HS cell line, LI90, was grown to 70–80% confluency, medium was changed to serum-free DMEM for 48 h, and the supernatant was concentrated with Amicon Ultra filters for 3 kDa (Millipore, MA, USA). Protein content of the concentrated HS cell-conditioned media (HS-CM) was determined by Bradford assay, and aliquots were stored at −80°C until use. Conditioned media were similarly prepared from the two cholangiocarcinoma cell lines (CC-CM), HuCCT-1 and RBE.

Proliferation Assay

LI90 cells were seeded at 5,000 per well in 96-well plates and cultured overnight in DMEM/10% FBS. Medium was changed to serum-free DMEM, and concentrated conditioned medium in which cholangiocarcinoma cells had been incubated (CC-CM) was added to cells at varying concentrations (0.05, 0.1, 0.5 μg/μl). Serum-free DMEM was added to control wells. Similarly, HuCCT-1 or RBE cells were seeded at 5,000 per well in 96-well plates and cultured overnight in DMEM/10% FBS. Medium was changed to serum-free DMEM, and concentrated HS-CM was added to cells at varying concentrations (0.05, 0.1, 0.5 μg/μl). Cell growth was analyzed after 48 h by adding the WST-8 reagent (Dojin Laboratories, Kumamoto, Japan) and taking the spectrophotometric reading 2 h later.

Invasion Assay

Biocoat Matrigel-coated invasion chambers (BD Biosciences, CA, USA) were used to examine cell invasiveness. In brief, 5×10^4 HuCCT-1 or RBE cells in 500 μl serum-free medium were added to the upper chamber. Medium containing 10% FBS or concentrated HS-CM (0.05, 0.1, 0.25, 0.5 μg/μl) was added to the lower chamber. Serum-free medium was added to the lower chamber of control wells. The cells were allowed to invade the Matrigel for 24 h at 37°C in 5% CO_2 atmosphere. The noninvading cells on the upper surface of the membrane were removed with a cotton swab. Cells were fixed in methanol, stained with 1% toluidine blue, and air-dried. Invading cells in three adjacent microscope fields for each membrane were counted at 20× magnification.

Immunocytochemistry

To demonstrate the effects of cholangiocarcinoma on LI90 cells, LI90 cells were seeded on glass coverslips in DMEM/10% FBS and incubated for 8 h. Medium was changed to concentrated CC-CM (0.25 μg/μl), and cells were incubated for 12 h. Serum-free DMEM was used as control. CC-CM was collected from HuCCT-1 or RBE cells. The cells were fixed and stained by α-SMA. For details, see the Supplementary Information.

Western Blot Analysis

To evaluate activation of HS cells in the presence of CC-CM, LI90 cells were seeded and grown in 6-cm dishes in DMEM/10% FBS for 8 h. Medium was changed to concentrated CC-CM (0.5 μg/μl) medium, or serum-free medium, and incubated for 12 h. To evaluate activation of the mitogen-activated protein kinase (MAPK) and Akt pathways in HS-CM, HuCCT-1 cells were grown in six-well plates in DMEM/10% FBS to 70% confluency. Cells were serum-starved overnight, and treated with HS-CM (0.5 μg/μl) for 0–120 min. The cells were lysed and

analyzed by Western blotting. For details, see the Supplementary Information.

HUVEC Tube Formation Assay

To investigate which cells played a greater role in angiogenic factor production, not only CMs from HS cells (HS-CM) and tumor cells (CC-CM) but also secondary CMs were prepared from tumor-stimulated HS cells (CC-HS-CM), and HS cell-stimulated tumor cells (HS-CC-CM); for details, see Supplementary Fig. 1. HUVECs (1×10^4 cells/well) were suspended in a mixture of CM (100 μl) and EGM-2 medium (100 μl) with 0.5% FBS, and seeded on 50 μl Matrigel in 96-well culture plates. Serum-free DMEM (100 μl) in place of conditioned media was used as control. After incubation for 12 h, photographs of each well were taken. The total capillary tube length and branching points in three random view-fields per well were examined, and the values were averaged.

Apoptosis Assay against Chemotherapy

HuCCT-1 cells were seeded in eight-well chamber slides (1×10^5 per well) (Nunc, NY, USA) in RPMI with 10% FBS. After incubation overnight, cells were washed, and medium was changed to RPMI with or without HS-CM (0.5 μg/μl). Cells were treated with CDDP, 5-FU, or gemcitabine chemotherapeutic reagents, or vehicle. After 24 h, apoptotic cells were analyzed with terminal deoxyribonucleotidyl transferase-mediated dUTP nick end labeling (TUNEL) assay (Promega, WI, USA), and nuclei were stained with Mayer's hematoxylin. The ratio of apoptotic cells was calculated as: (number of cells positive for TUNEL/number of nuclei stained with Mayer's hematoxylin) × 100. Experiments were performed in triplicate, and 10 random fields were counted for each condition.

Subcutaneous Injection Model of Cholangiocarcinoma

All animal experiments were reviewed and approved by the University of Kumamoto Institutional Animal Care and Use Committee. Female athymic nude mice (BALB/c nu/nu; age, 6–8 weeks) were grouped into three sets of five mice. The five mice in each set were injected subcutaneously with one of the following: (a) 1.5×10^6 LI90 cells/100 μl PBS, (b) 3×10^6 HuCCT-1 cells/100 μl PBS, or (c) mixture of HuCCT-1 cells (3×10^6) + LI90 cells (1.5×10^6) in 100 μl PBS. Mice were sacrificed 7 weeks after injection, the tumors were removed, and the tumor weights were recorded. Tumors were processed for histological examination.

Immunohistochemistry

To investigate the influence of HS cells on tumorigenesis in mice, we performed immunohistochemical study using α-SMA for evaluating myofibroblasts and CD31 for evaluating angiogenesis. For details, see the Supplementary Information.

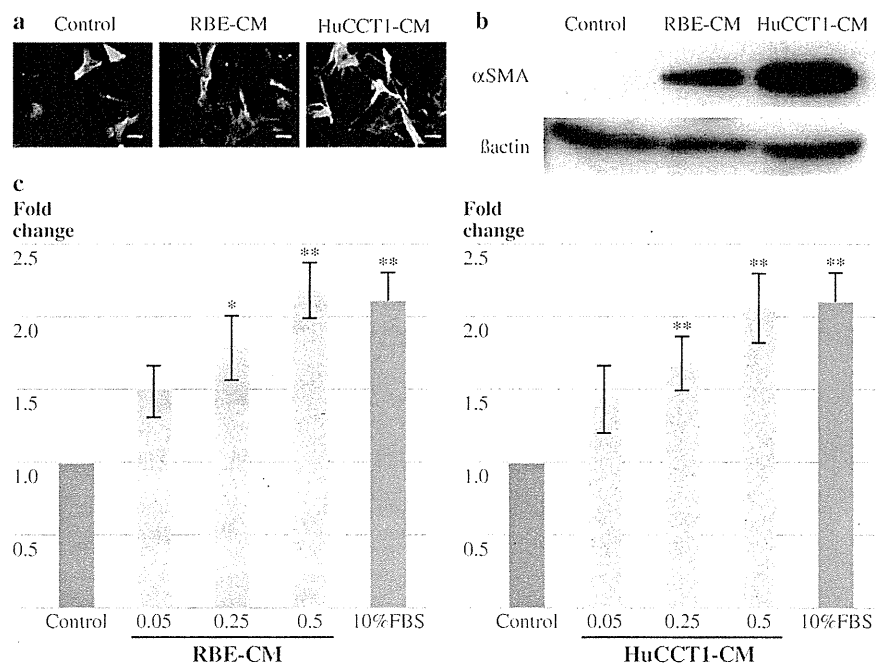

FIG. 1 Effect of CC-CM on HS cell phenotype. **a** Immunohistochemical staining for α-SMA of HS cells. RBE-CM or HuCCT1-CM was added to HS cells, and the cell morphology was compared with that of HS cells in serum-free medium; bar, 100 μm. **b** CC-CM-induced α-SMA expression was evaluated using Western blotting. **c** HS cell proliferation was measured in the presence of RBE-CM or HuCCT1-CM. Columns, mean of three experiments. * $P < 0.05$ and ** $P < 0.01$ versus serum-free media control

Cytokine Expression Analysis

To clarify secreted proteins induced by the interaction of cancer cells and stromal cells, we used a coculture model. Cytokine concentrations in conditioned medium were quantified using a cytokine array (R&D, MN, USA) as per the manufacture's protocol. For details, see the Supplementary Information.

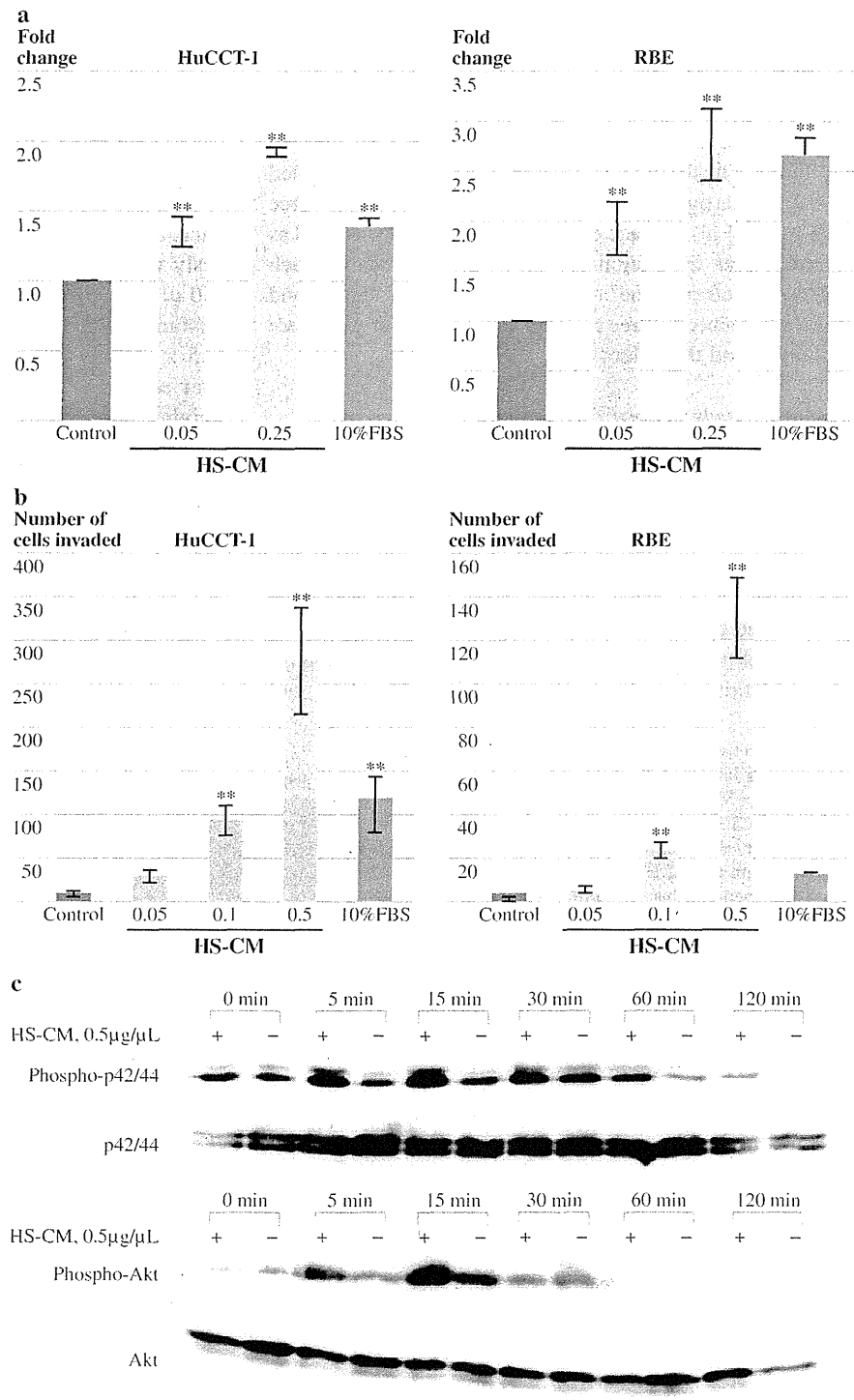

FIG. 2 Effect of HS-CM on cholangiocarcinoma cell phenotype. HS-CM (μg/μl) was added to RBE or HuCCT-1 cholangiocarcinoma cells. **a** Tumor cell proliferation was measured by 3-(4,5-dimethylthiazol-2-yl)-2,5-diphenyltetrazolium bromide (MTT) assay at 48 h. **b** Tumor cell invasion was evaluated at 24 h by using a Matrigel chamber assay. **c** Protein lysates from HuCCT-1 cells treated with HS-CM (0.5 μg/μl) were analyzed for Erk1/2 and Akt activation by Western blotting at various time points. Columns, mean of three experiments. ** $P < 0.01$ versus serum-free media control

Statistical Analysis

Statistical analysis was performed using the StatView J-5.0 program (Abacus Concepts Inc., Berkeley, CA, USA). Comparisons were carried out using Student's t test, and P values <0.05 were considered statistically significant. We analyzed using analysis of variance (ANOVA) followed by Tukey–Kramer post hoc test to compare multiple samples, with significance level of 0.05.

RESULTS

CC-CMs Induce Activation and Proliferation of HS Cells

To confirm the activation of HS cells by cholangiocarcinoma, two CC-CMs were added to HS cells, and the resulting changes in morphology and proliferation were compared with the serum-free medium control. Compared with the serum-free control, addition of CC-CMs produced by two cholangiocarcinoma cell lines altered the morphology of HS cells to that of myofibroblasts (Fig. 1a) and increased expression of α-SMA, a known marker of active HS cells (Fig. 1b). CC-CMs induced a dose-dependent increase in HS cell proliferation compared with serum-free medium controls (Fig. 1c).

HS Cells Stimulate Cholangiocarcinoma Cell Proliferation and Invasion

Addition of HS-CM to RBE cells increased tumor cell proliferation as compared with the proliferation in the case of serum-free medium controls (Fig. 2a). The effect was dose dependent, and a significant increase in proliferation compared with serum-free medium control wells was observed at 0.5 μg/μl (278 ± 35% of control; $P < 0.01$). The maximum effect of HS-CM on cell proliferation was greater on RBE cell proliferation than HuCCT1 cell proliferation, and was equal to the effect of 10% FBS (Fig. 2a). HS-CM also induced dose-dependent increases

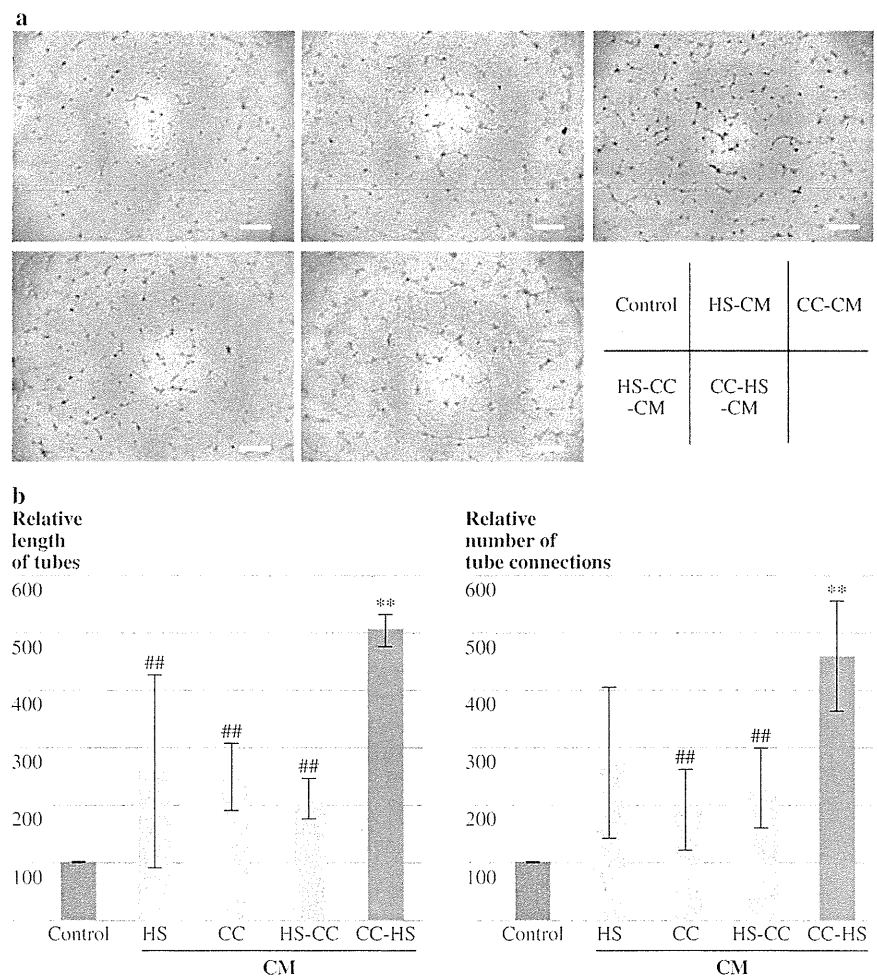

FIG. 3 The interaction of tumor and stromal cells induces HUVEC tube formation. **a** Representative photographs of HUVEC culture in Matrigel (12 h); bar, 100 μm. **b** HUVECs were treated with (a) HS-CM, (b) CC-CM, (c) secondary CM of RBE cells that were stimulated with the primary CM of HS cells (HS-CC-CM), and (d) secondary CM of HS cells that were stimulated with the primary CM of RBE cells (CC-HS-CM). Serum-free medium was used in place of CM as control; bar, μm. The relative length and number of connections are shown. ** $P < 0.01$ versus serum-free media control, ## $P < 0.01$ versus CC-HS-CM

in HuCCT-1 and RBE cell invasion (Fig. 2b). HuCCT-1 invasion was significantly induced with as little as 0.05 μg/μl HS-CM. The maximum dose (0.5 μg/μl HS-CM) stimulated a 25.3-fold increase, and the minimum dose (0.05 μg/μl HS-CM) stimulated a 2.8-fold increase in HuCCT-1 invasion compared with serum-free medium ($P < 0.0001$). The maximum dose of 0.5 μg/μl HS-CM resulted in HuCCT-1 invasion at a higher level than that in the medium containing 10% FBS (278 ± 62 versus 119 ± 25; $P < 0.001$).

Factors Secreted from HS Cells Stimulate Activation of MAPK and Akt Pathways in Tumor Cells

To determine signaling pathways that may be involved in the tumor-promoting effects of HS cells, HuCCT-1 tumor cells treated with HS-CM were examined for activation of MAPK and Akt by Western blotting. Increased phosphorylation of Erk1/2 was observed in cells treated with HS-CM compared with control cells from 5 to 120 min after treatment (Fig. 2c). Similarly, increased levels of phosphorylated Akt were observed from 5 to 60 min after stimulation with HS-CM.

Interaction between HS and Cholangiocarcinoma Cells Promotes HUVEC Tube Formation

We examined whether the interaction of HS cells and tumor cells induced angiogenesis in vitro using the HUVEC tube formation assay. HUVECs formed a network of capillary-like structures after 18 h of culture in Matrigel (Fig. 3a). CC-HS-CM significantly accelerated tube formation, in comparison with HS-CM or CC-CM, and the length and branching points of HUVEC tubes increased by 5.1 and 4.6 times, respectively (Fig. 3b). On the other hand, HUVEC tubes induced by treatment with HS-CC-CM were similar to those of either HS-CM or CC-CM (Fig. 3a, b). This indicated that tube formation was stimulated by the tumor cell-induced secretions of HS cells, but not by the HS cell-induced secretions of tumor cells. This is consistent with previous reports showing that

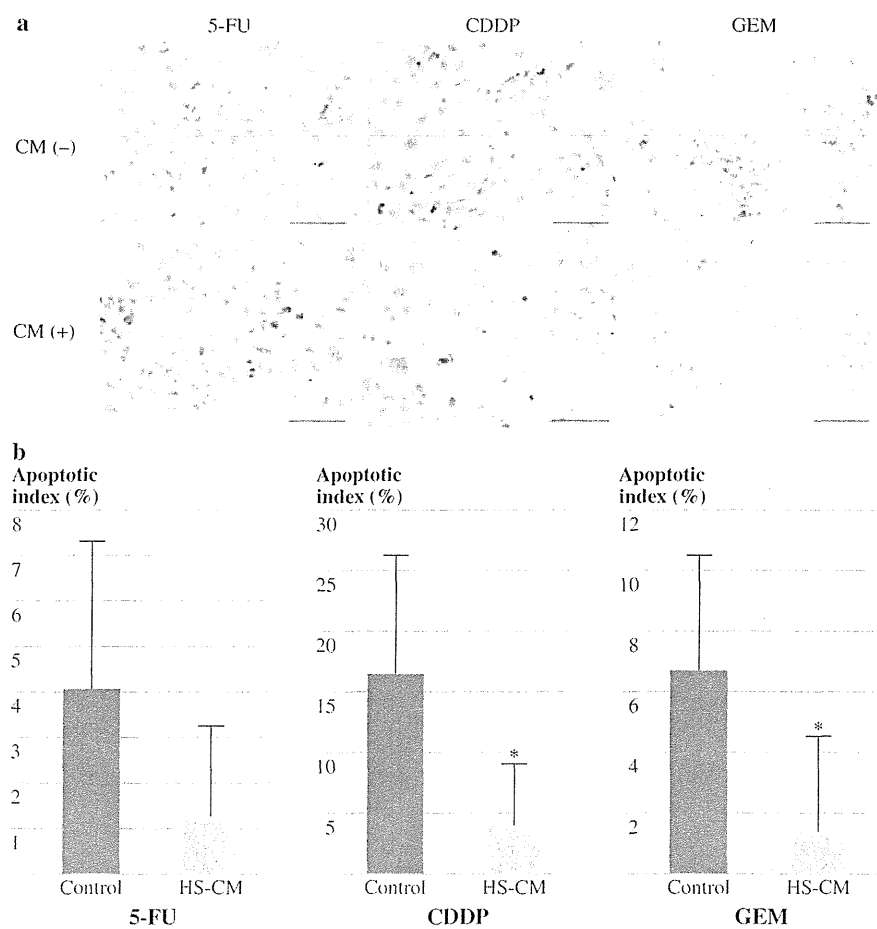

FIG. 4 Antiapoptotic effect of HS cells on cholangiocarcinoma cells against chemotherapy. HuCCT-1 cells were treated with 5-FU (500 μg/ml), CDDP (50 μg/ml), or gemcitabine (500 μg/ml) with or without HS-CM (0.25 μg/μl) for 24 h. **a** Apoptosis was detected using TUNEL assay, and cell nuclei were stained with Mayer hematoxylin. **b** Percentage of apoptotic cells was determined in five random fields for each condition. * $P < 0.05$

tumor cells stimulated fibroblasts to produce angiogenic factors in the indirect tumor–stromal cell interaction model.[14,15]

HS Cells Inhibit the Effects of Chemotherapy against Cholangiocarcinoma Cells

Addition of HS-CM to HuCCT-1 cells treated with 5-FU (500 μg/ml), CDDP (50 μg/ml), or gemcitabine (500 μg/ml) resulted in an inhibition of apoptosis (Fig. 4a). The percentage of apoptotic cells treated by 5-FU, CDDP, or gemcitabine in serum-free medium were 4.1% ± 3.2%, 16.4% ± 4.1%, and 6.7% ± 1.4% versus 1.2% ± 2.1%, 4.1% ± 5.2%, and 1.4% ± 3.2% with addition of HS-CM ($P = 0.134$, 0.038, and 0.045, respectively; Fig. 4b). No significant differences were observed in total cell number in cells treated with chemotherapeutic reagents, such as 5-FU, CDDP, or gemcitabine, with or without the addition of HS-CM.

Co-injection of HS Cells and Tumor Cells Induces Tumor Progression in an In Vivo Subcutaneous Injection Model of Cholangiocarcinoma

Palpable tumors were not detected in the mice injected with HS cells alone, suggesting that HS cells do not have tumorigenic potential. However, a significant increase in tumor volume was observed in the HuCCT-1 and LI90 mixed group versus the HuCCT-1 group when all data were analyzed ($n = 5$ per group) (Fig. 5a, b). The tumor weight at 6 weeks was also significantly greater in the mixed group than in the HuCCT-1 group. These findings suggest that the presence of HS cells accelerated the growth of cholangiocarcinoma. One mouse in the mixed group had a subcutaneous hemorrhage after cell injection, resulting in the disappearance of tumor cells at final evaluation. This outcome was ascribed to human error. To analyze whether in vivo tumor formation induced by HS cell co-injection is caused by increased myofibroblasts or increased angiogenesis, we performed immunohistochemical analysis. Mixed tumors of HuCCT1 and LI90 did not show more intense staining of α-SMA and CD31 than tumors formed by HuCCT1 cells alone (Fig. S2).

Co-culture of HS Cells and Cholangiocarcinoma Cells Induced Production of IL-1α, C5a, IL-1β, and G-CSF

We assessed the mediators secreted by cells in monoculture and coculture by performing cytokine arrays on conditioned media samples (Fig. 6a). Of the 36 proteins examined, 20 were detectable at the limits of sensitivity of this assay (Fig. 6b, c). Proteins were considered to be increased if they were present in the

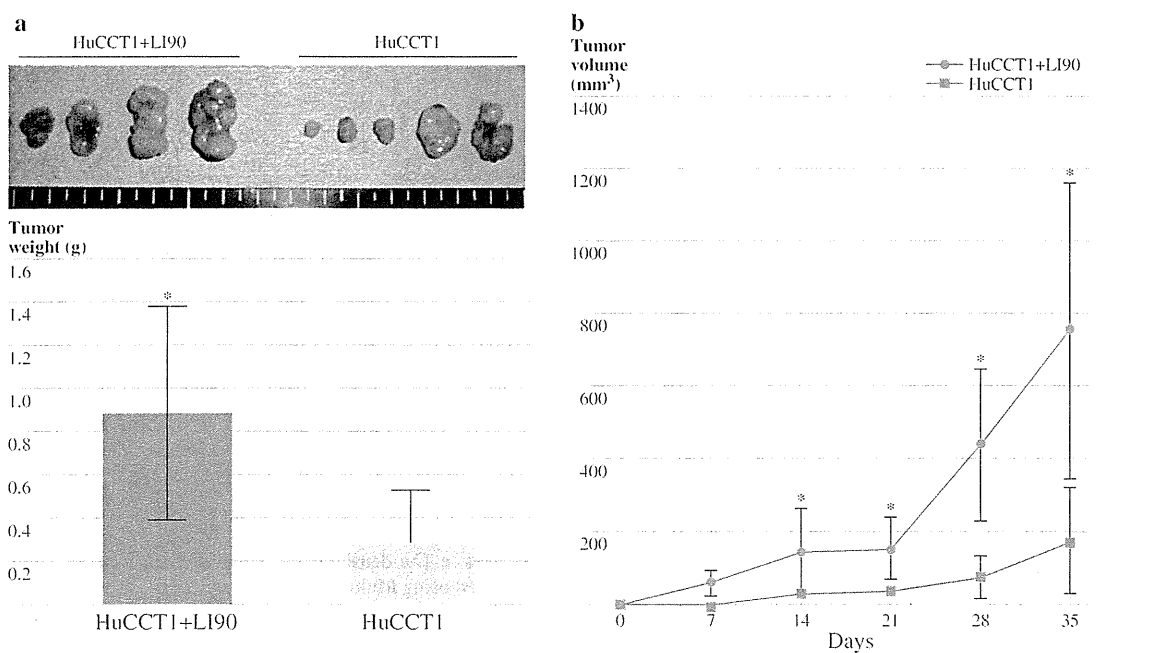

FIG. 5 Subcutaneous co-injection of HS cells with HuCCT-1 cells in nude mice resulted in increased tumor size and weight. **a** Mice were sacrificed after 35 days, and the resulting tumors were removed, photographed, and weighed (mean ± SD). * $P < 0.05$. **b** Tumor size was measured weekly, determined using a caliper rule. Tumor volume was calculated by using the formula $(a \times b \times c)/2$, where a and b are the short and long diameters of the tumors, respectively, and c is the thickness

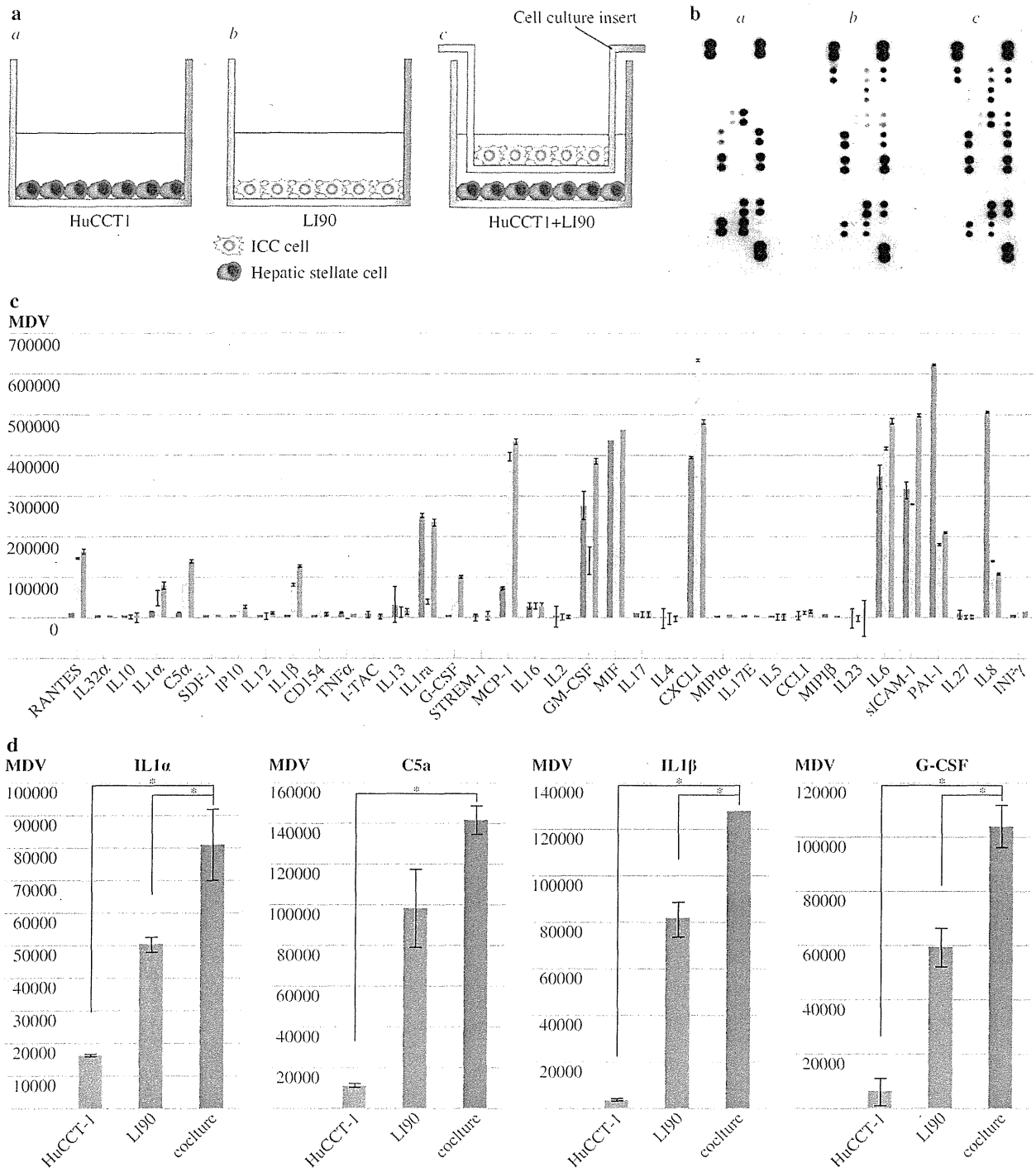

FIG. 6 Quantitative evaluation of cytokines and chemokines in conditioned media samples from monoculture and coculture based on cytokine arrays. **a** CM samples were prepared from (a) monocultured HuCCT-1, (b) monocultured LI90, and (c) cocultured HuCCT-1 and LI90. **b** Representative membrane arrays from three samples after development. A total of three membranes that included 36 molecules measured for duplicates were processed to generate data used in our analyses. **c** The densitometric value of each locus on the array was measured using Multi Gauge software (FUJIFILM, Japan). The value will be referred to as the mean densitometric value (MDV) of each cytokine. **d** The molecules IL-1α, C5a, IL-1β, and G-CSF were selected such that the value of coculture (c) was more than the total value of the two monocultures ($a + b$). * $P < 0.05$

coculture at a value that was greater than the total value of the two monocultures, and four proteins met this criterion: interleukin (IL)-1α, C5a, IL-1β, and granulocyte colony-stimulating factor (G-CSF). These proteins were detected at much lower level in the cancer cell monoculture than in the HS cell monoculture. Among these four cytokines, the level of IL-1α, IL-1β, and G-CSF was significantly different between the HS cell monoculture and coculture (Fig. 6c).

DISCUSSION

Tumor–stromal interaction is an important aspect of cancer progression that warrants further clarification. Many investigators have shown that CAFs, so-called myofibroblasts, play a pivotal role in tumor progression, and have studied CAFs for the purpose of stroma-targeted therapy.[19,20] We previously suggested that HS cells might promote cholangiocarcinoma progression, and the present study demonstrated the interaction of HS cells and cholangiocarcinoma cells in vitro and in vivo.[10] Consistent with our expectations, HS cells were activated by tumor cells and promoted the growth of them. The interaction of these cells in vitro and in vivo has never been investigated, and the current study supports the notion that HS cells may be CAFs in cholangiocarcinoma.

Previous studies focused on the role of stellate cells in pancreatic cancer, and various mechanisms were found.[5,11,13,21–23] Pancreatic stellate cells induced tumor growth and invasion, and inhibited chemotherapy-induced apoptosis in pancreatic cancer. Previous studies suggested that PDGF was the most important factor for stellate cell-induced tumor growth using a neutralizing antibody assay.[11,13] Similar to these reports, HS cells induced a dose-dependent increase in the proliferation and invasion of tumor cells in our study.

Several studies suggested that stellate cells influenced tumor response to chemotherapy in pancreatic cancer.[24,25] We hypothesized that HS cells behave like pancreatic stellate cells, and confirmed the antiapoptotic effect of HS cells on tumor cells using TUNEL assay. We used common clinical chemotherapeutic agents against cholangiocarcinoma, and determined that HS cells have an antiapoptotic effect on CDDP and gemcitabine treatments.

Interestingly, stromal cells are indispensable in tumor angiogenesis, and therefore antiangiogenic therapies must be aimed to target stromal cells as well as cancer cells.[14,15] We observed that tumor cells induced secretions in HS cells that stimulated tube formation, but this effect was not seen when we replaced tumor cells with stromal cells. This result emphasized the importance of stromal cells in angiogenesis.

The presence of HS cells significantly increased the tumor growth in vivo, and this supports the idea that HS cells provide an advantageous microenvironment for cholangiocarcinoma cells. We examined the amount of stromal component and the microvessel density in excised tumors, but we did not observe any differences between the tumor cell-only injection group and the co-injection group. LI90 cells are not immortalized, and their active lives are very limited. LX2 may be a better cell line for use in the tumor formation assay, or in other detailed in vivo analyses.

The current study identified three candidate molecules that may participate in the tumor–stromal interaction: IL-1α, IL-1β, and G-CSF. The significance of IL-1β in the tumor–stromal interaction has been reported.[16,26,27] Inflammation is one of the important aspects of cancer development, and CAFs are known to behave like myofibroblasts in the wound. Similarly, we believe to have found the same characteristics between hepatic stellate cells in carcinoma and those in damaged liver. Identification of the key characteristics of hepatic stellate cell for tumor development remains a problem for future study, and we would like to elucidate this issue using several candidate secreted proteins identified by the current study. We believe that these proteins may provide clues to therapeutic targets focusing on CAFs.

In conclusion, our data provide evidence that HS cells interact with tumor cells to promote tumor progression in cholangiocarcinoma in vitro and in vivo. Thus, HS cells may be a therapeutic target for inhibition of tumor–stromal interaction in cholangiocarcinoma.

ACKNOWLEDGMENT We thank Mr. Kikuchi K for kind advice regarding statistical analysis.

REFERENCES

1. DeOliveira ML, Cunningham SC, Cameron JL, et al. Cholangiocarcinoma: thirty-one-year experience with 564 patients at a single institution. *Ann Surg.* 2007;245:755–62.
2. Gores GJ. Cholangiocarcinoma: current concepts and insights. *Hepatology.* 2003;37:961–9.
3. Patel T. Increasing incidence and mortality of primary intrahepatic cholangiocarcinoma in the United States. *Hepatology.* 2001;33:1353–7.
4. Joyce JA, Pollard JW. Microenvironmental regulation of metastasis. *Nat Rev Cancer.* 2009;9:239–52.
5. Hwang RF, Moore T, Arumugam T, et al. Cancer-associated stromal fibroblasts promote pancreatic tumor progression. *Cancer Res.* 2008;68:918–26.
6. Olumi AF, Grossfeld GD, Hayward SW, et al. Carcinoma-associated fibroblasts direct tumor progression of initiated human prostatic epithelium. *Cancer Res.* 1999;59:5002–11.
7. Orimo A, Gupta PB, Sgroi DC, et al. Stromal fibroblasts present in invasive human breast carcinomas promote tumor growth and angiogenesis through elevated SDF-1/CXCL12 secretion. *Cell.* 2005;121:335–48.

8. Tsujino T, Seshimo I, Yamamoto H, et al. Stromal myofibroblasts predict disease recurrence for colorectal cancer. *Clin Cancer Res.* 2007;13:2082–90.
9. Friedman SL. Hepatic stellate cells: protean, multifunctional, and enigmatic cells of the liver. *Physiol Rev.* 2008;88:125–72.
10. Okabe H, Beppu T, Hayashi H, et al. Hepatic stellate cells may relate to progression of intrahepatic cholangiocarcinoma. *Ann Surg Oncol.* 2009;16:2555–64.
11. Vonlaufen A, Joshi S, Qu C, et al. Pancreatic stellate cells: partners in crime with pancreatic cancer cells. *Cancer Res.* 2008;68:2085–93.
12. Sato N, Maehara N, Goggins M. Gene expression profiling of tumor-stromal interactions between pancreatic cancer cells and stromal fibroblasts. *Cancer Res.* 2004;64:6950–6.
13. Bachem MG, Schunemann M, Ramadani M, et al. Pancreatic carcinoma cells induce fibrosis by stimulating proliferation and matrix synthesis of stellate cells. *Gastroenterology.* 2005;128: 907–21.
14. Guo X, Oshima H, Kitmura T, et al. Stromal fibroblasts activated by tumor cells promote angiogenesis in mouse gastric cancer. *J Biol Chem.* 2008;283:19864–71.
15. Noma K, Smalley KS, Lioni M, et al. The essential role of fibroblasts in esophageal squamous cell carcinoma-induced angiogenesis. *Gastroenterology.* 2008;134:1981–93.
16. Erez N, Truitt M, Olson P, et al. Cancer-associated fibroblasts are activated in incipient neoplasia to orchestrate tumor-promoting inflammation in an NF-kappaB-dependent manner. *Cancer Cell.* 2010;17:135–47.
17. Murakami K, Abe T, Miyazawa M, et al. Establishment of a new human cell line, LI90, exhibiting characteristics of hepatic Ito (fat-storing) cells. *Lab Invest.* 1995;72:731–9.
18. Xu L, Hui AY, Albanis E, et al. Human hepatic stellate cell lines, LX-1 and LX-2: new tools for analysis of hepatic fibrosis. *Gut.* 2005;54:142–51.
19. Mueller MM, Fusenig NE. Friends or foes—bipolar effects of the tumour stroma in cancer. *Nat Rev Cancer.* 2004;4:839–49.
20. Kalluri R, Zeisberg M. Fibroblasts in cancer. *Nat Rev Cancer.* 2006;6:392–401.
21. Apte MV, Park S, Phillips PA, et al. Desmoplastic reaction in pancreatic cancer: role of pancreatic stellate cells. *Pancreas.* 2004;29:179–87.
22. Omary MB, Lugea A, Lowe AW, Pandol SJ. The pancreatic stellate cell: a star on the rise in pancreatic diseases. *J Clin Invest.* 2007;117:50–9.
23. Vonlaufen A, Phillips PA, Xu Z, et al. Pancreatic stellate cells and pancreatic cancer cells: an unholy alliance. *Cancer Res.* 2008;68:7707–10.
24. Miyamoto H, Murakami T, Tsuchida K, et al. Tumor-stroma interaction of human pancreatic cancer: acquired resistance to anticancer drugs and proliferation regulation is dependent on extracellular matrix proteins. *Pancreas.* 2004;28:38–44.
25. Muerkoster S, Wegehenkel K, Arlt A, et al. Tumor stroma interactions induce chemoresistance in pancreatic ductal carcinoma cells involving increased secretion and paracrine effects of nitric oxide and interleukin-1beta. *Cancer Res.* 2004;64:1331–7.
26. Aoki H, Ohnishi H, Hama K, et al. Autocrine loop between TGF-beta1 and IL-1beta through Smad3- and ERK-dependent pathways in rat pancreatic stellate cells. *Am J Physiol Cell Physiol.* 2006;290:C1100–8.
27. Cheng CY, Hsieh HL, Sun CC, et al. IL-1 beta induces urokinase-plasminogen activator expression and cell migration through PKC alpha, JNK1/2, and NF-kappaB in A549 cells. *J Cell Physiol.* 2009;219:183–93.

Ann Surg Oncol (2011) 18:1110–1115
DOI 10.1245/s10434-010-1384-6

Annals of
SURGICAL ONCOLOGY
OFFICIAL JOURNAL OF THE SOCIETY OF SURGICAL ONCOLOGY

ORIGINAL ARTICLE – PANCREATIC TUMORS

Perioperative Intra-Arterial and Systemic Chemotherapy for Pancreatic Cancer

Hiroshi Takamori, MD[1], Keiichiro Kanemitsu, MD[1], Masahiko Hirota, MD[1], Osamu Ikeda, MD[2], Hiroshi Tanaka, MD[1], Toru Beppu, MD[1], Yasuyuki Yamashita, MD[2], Natsuo Oya, MD[3], and Hideo Baba, MD[1]

[1]Department of Gastroenterological Surgery, Graduate School of Medical Sciences, Kumamoto University, Kumamoto, Japan; [2]Department of Diagnostic Radiology, Graduate School of Medical Sciences, Kumamoto University, Kumamoto, Japan; [3]Department of Radiation Oncology, Graduate School of Medical Sciences, Kumamoto University, Kumamoto, Japan

ABSTRACT

Background. Even after curative resection of pancreatic cancer, there is a high probability of systemic recurrence. This indicates that subclinical metastases are already present at the time of operation. The purpose of this study was to assess the feasibility and outcomes of patients who received a novel multimodality therapy combining pancreatic resection and intraoperative radiation therapy (IORT) with pre- and postoperative chemotherapy for pancreatic cancer.

Methods. For eligible patients with pancreatic cancer, 5-FU was administered at a dose of 125 mg/m^2/day on days 1–5 every week as a continuous pancreatic and hepatic arterial infusion, and gemcitabine was infused intravenously at a dose of 800 mg/m^2 per day once per week for 2 weeks for preoperative chemotherapy. Pancreatic resection combined with IORT was performed 1 week after preoperative chemotherapy. Postoperative chemotherapy was performed in the same way as preoperative chemotherapy. We performed an intention-to-treat analysis for all enrolled patients.

Results. This study enrolled 44 patients. The most common toxicities were hematological and gastrointestinal events. Grade 3/4 hematological toxicities were observed during preoperative chemotherapy, although there were no grade 3/4 nonhematological events. Postoperative chemotherapy-related toxicities were more critical and frequent than preoperative ones. There were no pre- or postoperative chemotherapy-associated deaths. Median overall survival was 36.5 months with 30.5% overall 5-year survival.

Conclusions. This multimodality therapy is feasible and promises to contribute to survival. It should be evaluated in a phase III setting.

First Received: 25 February 2010;
Published Online: 3 November 2010

H. Takamori, MD
e-mail: h-takamori@fc.kuh.kumamoto-u.ac.jp

Pancreatic adenocarcinoma remains a lethal disease, with an overall 5-year survival rate ranging from 0.4 to 5%.[1,2] Even after curative resection of pancreatic cancer, there is a high probability of systemic and/or local recurrence.[3–5] This indicates that subclinical metastases are already present in most patients at the time of operation, even if preoperative radiological imaging or intraoperative examination revealed no metastatic lesions. Therefore, a multimodality strategy, including not only local control but also treatment of micrometastases, is required for patients with pancreatic cancer. For local control, beginning in 1984 we introduced extended radical pancreatectomy combined with intraoperative radiation therapy (IORT).[6] This approach provided the best control of local recurrence, but there was no survival benefit because of blood-borne metastases.[5] To treat unresectable pancreatic cancer, we introduced a combination of chemotherapy using 5-fluorouracil (5-FU) pancreatic and hepatic arterial continuous infusion and systemic gemcitabine administration; this combined therapy was well tolerated, with a 1-year survival rate of 50.9%.[7]

We studied a novel multimodality therapy combining pancreatic resection and IORT with pre- and postoperative chemotherapy using 5-FU intra-arterial continuous infusion and systemic gemcitabine administration in patients with potentially resectable pancreatic cancer. The purpose of this study was to evaluate the feasibility and outcomes of this multimodality therapy.

PATIENTS AND METHODS

Patients

All patients were advised of the investigational nature of the study and gave their written, informed consent to participate before the beginning of the study. All patients underwent a standard pretreatment evaluation that included a physical examination, a thin-section, contrast-enhanced, multiphase spiral computed tomography (CT) of the abdomen, and ultrasonography. The absence of liver metastasis was confirmed by CT during arterial portography combined with CT-assisted hepatic arteriography (CTAP + CTHA), as described previously.[8] The absence of lung metastasis was confirmed by chest CT. The protocol required patients with potentially resectable disease as assessed by a physical examination and the following objective radiographic criteria: (1) no evidence of remote metastases; (2) no evidence of tumor extension to the celiac axis or the superior mesenteric artery. We included only patients in whom it was technically possible to resect and reconstruct the superior mesenteric vein (SMV) or the portal vein (PV), if the tumor involved SMV or PV. We excluded cases in which the tumor was 1 cm or smaller in diameter, because of the very low possibility of systemic spreading of the disease. Patients were required to have an Eastern Cooperative Oncology Group performance status of ≤ 2.

Perioperative Chemotherapy

The treatment schema is shown in Fig. 1. The pre- and postoperative chemotherapy consisted of the combination of 5-FU arterial continuous infusion and systemic gemcitabine administration. In all cases, the catheter for arterial infusion was introduced from the femoral artery under local anesthesia. After the closure of the distal tip of the catheter, a side hole was made at an appropriate site in the celiac axis to allow the distribution of 5-FU to both the pancreatic tumor and the liver preoperatively, and in the hepatic artery to distribute the drug to the whole liver postoperatively. An arterial port was implanted in the subcutaneous tissue. 5-FU was administered at a dose of 125 mg/m^2 per day on days 1–5 each week as continuous infusion through the arterial port for 2 weeks during preoperative chemotherapy and for 8 weeks during postoperative chemotherapy. Gemcitabine was infused intravenously for 30 min at a dose of 800 mg/m^2 once weekly for a total of 2 doses preoperatively and for a total of 18 doses postoperatively. The doses of these drugs were based on our preliminary results for the combination chemotherapy using 5-FU intra-arterial infusion and systemic gemcitabine for unresectable pancreatic cancer.[7]

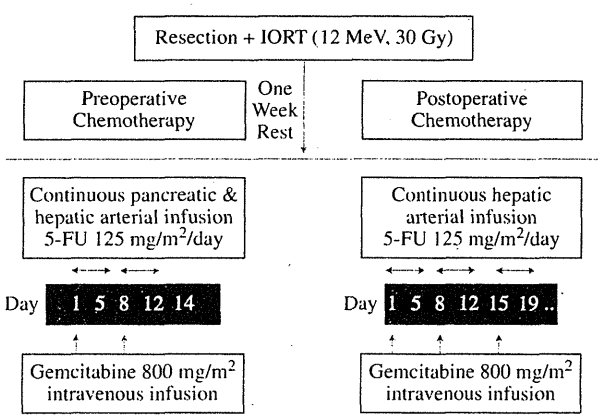

FIG. 1 Treatment schema. 5-FU was administered on days 1–5 every week as a continuous arterial infusion combined with gemcitabine infused once weekly for 2 weeks followed by pancreatic resection combined with IORT. Postoperative chemotherapy was performed in the same way as preoperative chemotherapy

In cases of grade 3 or higher toxicity according to the National Cancer Institute-Common Toxicity Criteria (NCI-CTC) version 3.0, drug infusion was interrupted until recovery. History, physical examination, and complete blood counts (CBCs) were repeated weekly before infusion of the drugs. Chemistry profiles were performed every 2 weeks. The catheter and port for arterial infusion were removed after the completion of intra-arterial infusion of 5-FU.

Surgery

Patients with cancer of the head of the pancreas underwent a substomach-preserving pancreaticoduodenectomy (SSPPD), a pylorus-preserving pancreaticoduodenectomy (PPPD), or a Kausch-Whipple resection: the last of these was performed if a tumor directly invaded the duodenum or antrum of the stomach, or if a distal gastrectomy had been performed before. Patients with cancer of the body or tail of the pancreas underwent a distal pancreatectomy. Patients underwent resection with reconstruction of SMV or PV if a tumor was thought during surgery to involve these vessels. For IORT, a dose of 30 Gy with a 12 MeV of electron beam was delivered to the operative field using a special pentagon applicator following dissection, as described previously.[6]

Hospital death was defined as death during hospitalization. Major surgical complications included any occurrence of anastomotic leak, postoperative intra-abdominal or gastrointestinal hemorrhage or fistula, intra-abdominal abscess, pneumonia, catheter-related sepsis, thromboembolic events, and reoperation. Pancreatic fistula was assessed according to an international study group (ISGPF) definition.[9]

Toxicity and Outcome Evaluation

Toxicities were graded according to NCI-CTC version 3.0. Survival was calculated from the day of surgery and estimated by the Kaplan–Meier method. The first site of disease recurrence was documented for outcome analysis.

All patients were evaluated every 3–4 months by physical examination as well as by chest and abdominal CT after surgery. For those without any recurrence after 2 years, follow-up was at 6-month intervals. Cytologic or histologic confirmation of disease recurrence was not required.

RESULTS

Patient Characteristics

From May 2001 through September 2008, 44 patients were enrolled in this study. The patients' characteristics are outlined in Table 1. The primary pancreatic lesion was located in the head in 33 patients, in the body in 9, and in the tail in 2. All patients underwent pancreatic resection. Pancreatic ductal adenocarcinoma was confirmed in all patients histologically. R0 resection was performed in 37 patients, R1 resection in 5 (11.4%), and R2 resection in 2 (4.5%). The median tumor size was 3 (range, 1.3–8.7) cm. Lymph node metastases were identified in 30 patients (68.2%), including para-aortic lymph node metastases in 3 patients. Resection and reconstruction of SMV or PV were necessary in 22 patients (50%), although 13 (29.5%) were proven to have histological portal invasion. Thirty-four patients received IORT after resection. All of the patients began postoperative chemotherapy after recovery from surgery, although 20 patients (45.5%) were completely treated according to the postoperative schedule. The mean pre- and postoperative doses of total 5-FU administered per patient were 2.8 and 5.2 g. The mean pre- and postoperative doses of total gemcitabine were 5.2 and 14.3 g.

TABLE 1 Patient characteristics

Characteristics	No. of patients	%
Total no. of patients	44	
Median age (yr)	65 (37–79)	
Male/female	26/18	
Site of primary lesion		
Head	33	75
Body	9	20.5
Tail	2	4.5
Pancreatectomy		
PPPD	16	36.4
SSPPD	13	29.5
PD	4	9.1
DP	11	25
Stage		
Ia	3	6.8
Ib	1	2.3
11a	10	22.7
11b	26	59.1
III	1	2.3
IV	3	6.8
Histologic differentiation		
Well	16	36.4
Moderately	22	50
Poorly	5	11.4
Adenosquamous	1	2.3
Tumor size (cm)		
1.0–2.0	6	13.6
2.1–4.0	33	75
>4.1	5	11.4
Nodal involvement		
Present	30	68.2
Absent	14	31.8
Portal vein invasion		
Present	13	29.5
Absent	31	70.5
Residual tumor		
R0	37	84.1
R1	5	11.4
R2	2	4.5

PPPD pylorus-preserving pancreaticoduodenectomy; *SSPPD* substomach-preserving pancreaticoduodenectomy; *PD* pancreaticoduodenectomy; *DP* distal pancreatectomy

Toxicities of Pre- and Postchemotherapy and Surgery

All 44 patients were included in the toxicity analysis. The overall toxicity profiles related to pre- and postoperative chemotherapy are outlined in Table 2. The most common toxicities were hematological and gastrointestinal events.

Nineteen patients (43.2%) experienced grade 3/4 neutropenia during preoperative chemotherapy. All preoperative chemotherapy-related toxicities abated after discontinuation of drug infusion. Forty-three patients underwent surgery 1 week after the completion of preoperative chemotherapy. Only one patient experienced a delay in surgery because of grade 4 neutropenia. Five major complications occurred in five patients after surgery, including grade C pancreatic fistula in two patients, intra-abdominal abscess in one, and cerebral infarction in one. Three patients recovered from complications by means of conservative therapies. One patient underwent reoperation for grade C pancreatic fistula. Hospital death was observed in one patient because of liver failure after intra-abdominal bleeding caused by pancreatic fistula.

TABLE 2 Pre- and postoperative chemotherapy-related grade 3/4 toxicities

	Preoperative	Postoperative
Hematological		
Anemia	0	4 (9.1)
Leukopenia	8 (18.2)	14 (31.8)
Neutropenia	19 (43.2)	24 (54.5)
Thrombocytopenia	2 (4.5)	3 (6.8)
Others		
Perforation of small intestine	0	1 (2.3)
Liver abscess	0	3 (6.8)
Cardiac ischemia/infarction	0	2 (4.5)
Renal dysfunction	0	1 (2.3)
Cholangitis	0	3 (6.8)
Appetite loss	0	1 (2.3)

Percentages are shown in parentheses

Toxicities are defined by NCI-CTC for Adverse Events v3.0

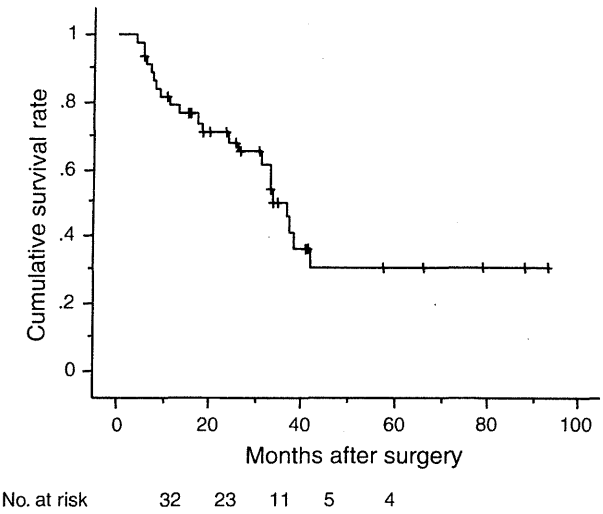

FIG. 2 Overall survival curve for all patients

Postoperative chemotherapy was initiated between 3 and 12 weeks after surgery. Twenty-four patients (54.5%) experienced grade 3/4 neutropenia during postoperative chemotherapy, although these toxicities abated after drug infusion was interrupted. Perforation of the small intestine in one patient occurred 1 year after pancreatic resection. This patient underwent emergency surgery and recovered. Grade 3/4 cardiac ischemia occurred in two patients and liver abscess in three patients (6.8%) during postoperative chemotherapy. No intra-arterial catheter-related toxicity occurred in any of the patients. Neither pre- nor postoperative chemotherapy-associated death was observed.

Survival and Outcome

The median follow-up period was 28.2 (range, 5.5–93.3) months. The 1, 3, and 5-year actuarial overall survival rates in all the patients were 78.8, 50.3, and 30.5%, respectively (Fig. 2). The median survival time was 36.5 months.

At last follow-up, 22 of the 44 patients (50%) had died. Seventeen (38.6%) had died as a result of recurrence. There were five (11.4%) non-cancer-related deaths, including one hospital death. Twenty-two patients (50%) remained alive. The median time of tumor recurrence was 24.0 months from the day of surgery. Liver metastases were observed in four patients (9.1%), peritoneal dissemination in six (13.6%), lung metastases in one (2.3%), pleural dissemination in one, bone metastases in one, and local recurrence in four (Table 3). Eight patients survived more than 32.3 months. The two patients with R2 resection died of peritoneal dissemination within 12 months.

TABLE 3 Outcomes after this multimodality therapy for patients with pancreatic cancer

	No.
Cancer deaths	17
Liver metastases	4
Lung metastases	1
Pleural dissemination	1
Peritoneal dissemination	6
Local recurrence	4
Bone metastases	1
Non-cancer-related deaths	5
Alive	22
Total	44

DISCUSSION

To our knowledge, this is the first report of perioperative intra-arterial and systemic chemotherapy for pancreatic cancer. This treatment was clearly operator-dependent. Grade 3/4 neutropenia was relatively frequent during perioperative chemotherapy, although the toxicities abated after interruption of drug infusion. Grade 3/4 nonhematological toxicities were observed during postoperative chemotherapy. Liver abscess occurred in three patients. This was thought to be influenced by regurgitated cholangitis, because all of the patients underwent hepaticojejunostomy after PD. Perforation of the small intestine occurred in one patient 3 months after completion of postoperative chemotherapy. Cardiac ischemia required hospitalization for two patients. However, the relationship between these events and chemotherapy was unclear. Toxicities were more critical and frequent during postoperative chemotherapy than during preoperative. Intra-arterial infusion was acceptable

for perioperative chemotherapy, because no catheter-related toxicity was observed.

Practical and theoretical advantages of preoperative treatment of pancreatic cancer were proposed as an early treatment for micrometastases and optimized patient selection for surgery.[10–12] Circulating tumor cells in the blood proved to be present in 28% of patients with pancreatic cancer, and the prevalence increased with tumor stages.[13] Moreover, complications, which occurred after 30–45% of major pancreatic resections, delayed the initiation of postoperative chemotherapy.[14,15] These are supported to introduce preoperative chemotherapy for pancreatic cancer.

The rationale for intra-arterial infusion of chemotherapeutic agents appears to be promising from the point of view of the drug-concentration response, because most liver metastases (>3 mm) have an arterial blood supply.[16,17] Locoregional adjuvant chemotherapy has been reported to have 3-year survival rates ranging from 48 to 54%, and lower recurrence rates of liver metastases ranging from 8 to 17% for pancreatic cancer compared with no-adjuvant studies.[3,4,18,19] This study also showed that liver metastases diminished to 9.1%, indicating that intra-arterial chemotherapy might be effective to prevent liver metastases.

We adopted pancreatic resection combined with IORT for local control in this series. Local recurrence was observed in only four patients (9.1%). Single-institution experiences suggest that local failure rates were lower in radiation groups (10–26%) than in no-radiation groups (50–80%).[20–24] This indicated that resection combined with IORT could provide good control of local recurrence.

Recently, a phase III randomized trial (CONCO 001 study) demonstrated that adjuvant gemcitabine significantly delayed the development of recurrence after resection of pancreatic cancer, with a median survival time of 22.1 months.[25] Evans et al. reported on a phase II trial of neoadjuvant gemcitabine-based chemoradiation for stage I/II pancreatic cancer.[26] The median survival time of 36.5 months in our study is similar to the 34 months in the Evans group trial despite a greater proportion of patients with node-positive (68.2%) and R2 resection (4.5%) in our study than in the Evans group trial. Because our perioperative chemotherapy is complicated, it will be necessary to clarify which adjuvant treatment is most effective for pancreatic cancer to simplify treatment.

In conclusion, this perioperative chemotherapy for pancreatic cancer is feasible and promises to contribute to survival. It should be evaluated in a phase III setting.

REFERENCES

1. Bramhall SR, Allum WH, Jones AG, Allwood A, Cummins C, Neoptolemos JP. Treatment and survival in 13560 patients with pancreatic cancer, and incidence of the disease, in the West Midlands: an epidemiological study. *Br J Surg.* 1995;82:111–5.
2. Jemal A, Siegel R, Ward E, Hao Y, Xu J, Murray T, Thun MJ. Cancer statistics, 2008. *CA Cancer J Clin.* 2008;58:71–96.
3. Griffin JF, Smalley SR, Jewell W, Paradelo JC, Reymond RD, Hassanein RE, Evans RG. Patterns of failure after curative resection of pancreatic carcinoma. *Cancer.* 1990;66:56–61.
4. Sperti C, Pasquali C, Piccoli A, Pedrazzoli S. Recurrence after resection for ductal adenocarcinoma of the pancreas. *World J Surg.* 1997;21:195–200.
5. Takamori H, Hiraoka T, Kanemitsu K, Tsuji T. Pancreatic liver metastases after curative resection combined with intraoperative radiation for pancreatic cancer. *Hepato-Gastroenterol.* 2004;51: 1500–3.
6. Hiraoka T, Uchino R, Kanemitsu K, et al. Combination of intraoperative radiation with resection of cancer of the pancreas. *Int J Pancreatol.* 1990;7:201–7.
7. Takamori H, Kanemitsu K, Tsuji T, et al. 5-Fluorouracil intra-arterial infusion combined with systemic gemcitabine for unresectable pancreatic cancer. *Pancreas.* 2005;30:223–6.
8. Takamori H, Ikeda O, Kanemitsu K, et al. Preoperative detection of liver metastases secondary to pancreatic cancer. Utility of combined helical computed tomography during arterial portography with biphasic computed tomography-assisted hepatic arteriography. *Pancreas.* 2004;29:188–92.
9. Bassi C, Dervenis C, Butturini G, et al. Postoperative pancreatic fistula: an international study group (ISGPF) definition. *Surgery.* 2005;138:8–13.
10. Evans DB, Rich TA, Byrd DR, et al. Preoperative chemoradiation and pancreaticoduodenectomy for adenocarcinoma of the pancreas. *Arch Surg.* 1992;127:1335–9.
11. Wayne JD, Abdalla EK, Wolff RA, Crane CH, Pisters PW, Evans DB. Localized adenocarcinoma of the pancreas: the rationale for preoperative chemoradiation. *Oncologist.* 2002;7:34–45.
12. Pisters PW, Wolff RA, Janjan NA, et al. Preoperative paclitaxel and concurrent rapid fractionation radiation for resectable pancreatic adenocarcinoma: toxicities, histologic response rates, and event-free outcome. *J Clin Oncol.* 2002;20:2537–44.
13. Z'graggen K, Centeno BA, Fernandez-del Castillo C, Jimenez RE, Werner J, Warshaw AL. Biological implications of tumor cells in blood and bone marrow of pancreatic cancer patients. *Surgery.* 2001;129:537–46.
14. Sohn TA, Yeo CJ, Cameron JT, et al. Resected adenocarcinoma of the pancreas–616 patients: results, outcomes, and prognosis indicators. *J Gastrointest Surg.* 2000;4:567–79.
15. Frederick WAI, Wolff RA, Crane CH. Preoperative (neoadjuvant) therapy for resectable adenocarcinoma of the pancreas. In: Evans DB, Pisters PWT, Abbruzzese JL, Pollock RE, editors. MD Anderson Solid Tumor Oncology Series. New York: Springer; 2001. p. 243–54.
16. Archer SG, Gray BN. Vascularization of small liver metastases. *Br J Surg.* 1989;76:545–8.
17. Ackermann NB. The blood supply of experimental liver metastases. IV. Changes in vascularity with increasing tumor growth. *Surgery.* 1974;75:589–96.
18. Ishikawa O, Ohigashi H, Sasaki Y, et al. Liver perfusion chemotherapy via both the hepatic artery and portal vein to prevent hepatic metastasis after extended pancreatectomy for adenocarcinoma of the pancreas. *Am J Surg.* 1994;168:361–4.
19. Beger HG, Gansauge F, Büchler MW, Link KH. Intraarterial adjuvant chemotherapy after pancreaticoduodenectomy for pancreatic cancer: significant reduction in occurrence of liver metastasis. *World J Surg.* 1999; 23:946–949.
20. Breslin TM, Hess KR, Harbison DB, et al. Neoadjuvant chemoradiotherapy for adenocarcinoma of the pancreas: treatment variables and survival duration. *Ann Surg Oncol.* 2001;8:123–32.
21. Spitz FR, Abbruzzese JL, Lee JE, et al. Preoperative and postoperative chemoradiation strategies in patients treated with

pancreaticoduodenectomy for adenocarcinoma of the pancreas. *J Clin Oncol.* 1997;15:928–37.
22. Tepper JE, Nardi G, Suit H. Carcinoma of the pancreas: review of MGH experience from 1963–1973. Analysis of surgical failure and implications for radiation therapy. *Cancer.* 1976;37:1519–25.
23. Kayahara M, Nagakawa T, Ueno K, Ohta T, Takeda T, Miyazaki I. An evaluation of radical resection for pancreatic cancer based on the mode of recurrence as determined by autopsy and diagnostic imaging. *Cancer.* 1993;72:2118–23.
24. Whittington R, Bryer MP, Haller DG, Solin LJ, Rosato EF. Adjuvant therapy of resected adenocarcinoma of the pancreas. *Int J Radiat Oncol Biol Phys.* 1991;21:1137–43.
25. Oettle H, Post S, Neuhaus P, et al. Adjuvant chemotherapy with gemcitabine vs observation in patients undergoing curative-intent resection of pancreatic cancer. A randomized controlled trial. *JAMA.* 2007;297:267–77.
26. Evans DB, Varadhachary GR, Crane CH, et al. Preoperative gemcitabine-based chemoradiation for patients with resectable adenocarcinoma of the pancreas. *J Clin Oncol.* 2008;26: 3496–502.

NO donor and MEK inhibitor synergistically inhibit proliferation and invasion of cancer cells

SATOSHI FURUHASHI[1], HIROKI SUGITA[1,2], HIROSHI TAKAMORI[1], KEI HORINO[1], OSAMU NAKAHARA[1], HIROHISA OKABE[1], KEISUKE MIYAKE[1], HIROSHI TANAKA[1], TORU BEPPU[1] and HIDEO BABA[1]

[1]Department of Gastroenterological Surgery, Graduate School of Medical Sciences, Kumamoto University, 1-1-1 Honjo, Kumamoto 860-8556; [2]Department of Surgery, Kumamoto City Municipal Hospital, 1-1-60 Koto, Kumamoto 862-8505, Japan

Received August 27, 2011; Accepted October 3, 2011

DOI: 10.3892/ijo.2011.1243

Abstract. Nitric oxide (NO) shows tumoricidal activity. We had previously reported that NO downregulates the phosphatidylinositol-3-kinase/Akt pathway, but upregulates the MEK/ERK pathway downstream of growth factor signaling. We hypothesized that NO donor and MEK inhibitor in combination synergistically inhibit the viability of cancer cells compared to either NO donor or MEK inhibitor alone. We determined the effects of S-nitrosoglutathione (GSNO, NO-donor) and U0126 (MEK inhibitor) on insulin-like growth factor-I (IGF-I) and epidermal growth factor (EGF) signaling, proliferation and invasion in cancer cell lines. GSNO inhibits phosphorylation of IGF-I receptor (IGF-IR), EGF receptor (EGFR) and Akt, but upregulates ERK1/2 phosphorylation in MIAPaCa-2 and HCT-116 cells after stimulation by IGF-I and EGF. On the other hand, U0126 inhibits phosphorylation of ERK1/2, but upregulates phosphorylation of IGF-IR and EGFR in MIAPaCa-2 and HCT-116 cells. The combination of GSNO and U0126 downregulates phosphorylation of IGF-IR, EGFR, Akt and ERK1/2 after stimulation by IGF-I and EGF. GSNO as well as U0126, inhibits the proliferation of MIAPaCa-2, HCT-116, Panc-1, MCF-7, HT-29 and AGS cells in a dose-dependent manner. GSNO and U0126 in combination synergistically inhibit proliferation and invasion of cancer cells. These results indicate that the combined treatment of NO donor and MEK inhibitor may be promising in cancer therapy.

Correspondence to: Dr Hiroki Sugita or Dr Hideo Baba, Department of Gastroenterological Surgery, Graduate School of Medical Sciences, Kumamoto University, 1-1-1 Honjo, Kumamoto 860-8556, Japan
E-mail: sugitaf@ba2.so-net.ne.jp
E-mail: hdobaba@kumamoto-u.ac.jp

Abbreviations: IGF-IR, IGF-I receptor; EGF, epidermal growth factor; EGFR, EGF receptor; NO, nitric-oxide; IRS-1, insulin receptor substrate-1; PI3K, phosphatidylinositol-3-kinase; GSNO, S-nitrosoglutathione; ERK, extracellular signal-regulated kinase; PTC, papillary thyroid carcinoma

Key words: nitric oxide, MEK, insulin-like growth factor receptor, epidermal growth factor receptor, Akt, extracellular signal-regulated kinase, cancer proliferation, cancer invasion, pancreatic cancer, colon cancer

Introduction

Insulin-like growth factor (IGF) and epidermal growth factor (EGF) signaling play a key role in cancer proliferation and invasion (1-5). IGF-I and EGF bind to IGF-I receptor and EGF receptor and then phosphorylate the tyrosine of the cognate receptors. Insulin receptor substrate (IRS)-1, an adaptor protein, exists mainly in the cytosol, and binds to phosphorylated IGF-IR, resulting in phosphorylation and activation of IRS-1. IRS-1 and EGF receptor (EGFR) transduce phosphatidylinositol-3-kinase (PI3K), which in turn activates further downstream components, including Akt. Alternatively, phosphorylated and activated EGFR and IRS-1 can also bind to another adaptor protein, Grb-2, which activates the MEK/ERK pathway, another major IGF and EGF signaling cascade parallel to the PI3K/Akt pathway (6,7).

Recent studies have shown that nitric-oxide (NO) plays a role in the posttranslational modification of proteins (8-11). Controversial results have been reported regarding the roles of NO in cancer. Recent papers reported that endogenous NO promotes oncogenesis and angiogenesis in various cancers (12,13). In contrast, other studies have shown that NO inhibits cell proliferation and induces apoptosis in various cells including cancer cells, *in vitro* and *in vivo* (14-21). These studies suggest that NO can act either as a tumor suppressor or as a tumor enhancer depending on cell type and the level of NO in the cells. However, the molecular mechanism underlying the inhibitory effects of NO on cancer viability, remains unclear. We have reported that NO inhibits cancer cell proliferation and invasion through downregulation of IRS-1 protein, resulting in inhibition of the PI3K/Akt pathway (14). In contrast, NO enhances nitrosylation and activates N-Ras and H-Ras proteins (22). Members of the Ras family of small GTPase proteins including K-Ras, N-Ras, and H-Ras, play central roles in the transduction of growth factor signals (23). Thus, NO downregulates the PI3K/Akt pathway, but upregulates the MEK/ERK pathway. Therefore, we hypothesized that the combination of NO donor and MEK inhibitor synergistically inhibits the proliferation and invasion of cancer cells

compared to either NO donor or MEK inhibitor alone. In the present study, we demonstrated that combination treatment of NO donor and MEK inhibitor shows greater inhibitory effects on the proliferation and invasion of cancer cells compared to either MEK inhibitor or NO donor alone, which are associated with the inhibition of both the PI3K/Akt and MEK/ERK pathways. These data provide new insight into the molecular basis underlying the regulation of cancer viability.

Materials and methods

Materials. S-nitrosoglutathione (GSNO) and U0126 were purchased from Calbiochem (San Diego, CA). Recombinant IGF-I and EGF were purchased from Peprotech (London, UK). Antibodies against phospho-Tyr 1135/1136 IGF-I Rβ, phospho-Tyr1068EGFR, phospho-Ser 473 Akt, phospho-ERK1/2, IGF-IR, EGFR, Akt, and ERK1/2 were purchased from Cell Signaling Technology (Beverly, MA).

Cell culture. MIAPaCa-2, HCT-116, Panc-1, MCF-7, HT-29 and AGS cells were obtained from the American Type Culture Collection (Manassas, VA), and were maintained in Dulbecco's modified Eagle's medium (DMEM) and RPMI-1640 medium supplemented with 10% fetal bovine serum (FBS) at 37˚C in a humidified atmosphere of 5% CO_2.

Cell lysis. Cells were lysed with cell lysis buffer [50 mM Tris-HCl (pH 7.6), 150 mM NaCl, 10 mM sodium fluoride, 2 mM sodium vanadate, 1 mM PMSF, 10 μg/ml aprotinin, 10 μg/ml leupeptin, 1 mM DTT, and 1% NP-40]. Following incubation on ice for 30 min, lysate samples were centrifuged at 13,000 g for 30 min. Aliquots of the supernatant containing equal amounts of protein, determined using Lowry assay, were subjected to immunoblotting followed by sodium dodecyl sulfate-polyacrylamide gel electrophoresis (SDS-PAGE).

Immunoblotting. A total of 20 μg of each protein sample was mixed with 5X sample buffer including 10% β-mercaptoethanol and the mixture was boiled for 5 min. The total cellular protein extracts were separated on 10% SDS polyacrylamide gels. The extracts were electrophoretically transferred onto nitrocellulose membranes (Bio-Rad, Hercules, CA), the membranes were blocked with 5% nonfat dried milk for 2 h at room temperature, and incubated with primary antibody for either 2 h at room temperature or overnight at 4˚C. This was followed by incubation with secondary antibody conjugated with anti-rabbit or mouse IgG antibody peroxidase for 2 h at room temperature. Detection was done with an enhanced chemiluminescence (ECL) reagent (GE Healthcare, Piscataway, NJ). Bands of interest were scanned by using Colorio GT-X970 (Epson, Tokyo, Japan) and were quantified with NIH Image 1.62 software (NTIS, Springfield, VA).

Cell proliferation assay. The mixture of GSNO (NO donor), U0126 (MEK inhibitor) and 100 μl of medium containing $5x10^3$ cancer cells was added to each well (of a 96-well plate). Cell proliferation assay was performed using Cell Counting kit-8 containing 2-(2-methoxy-4-nitrophenyl)-3-(4-nitrophenyl)-5-(2,4-disulfophenyl)-2H-tetrazolium (WST-8) (Dojin Laboratories, Kumamoto, Japan) after the incubation for 72 h. At the end of each experiment, the cell proliferation reagent WST-8 was added to each well and the plates were incubated at 37˚C for 2 h. Optical density (OD) (A450 nm) was measured using an automatic microplate reader (Molecular Devices, Sunnyvale, CA). Each experiment was performed in triplicate.

Invasion assay. The invasive activities of cultured MIAPaCa-2 and HCT-116 cells were assayed using BD BioCoat Matrigel invasion chambers (BD Biosciences, Bedford, MA). MIAPaCa-2 cells were initially seeded on a 24-well plate at a density of $5x10^4$ cells/well and cultured in DMEM/10% FBS, in the presence of 1% glutamine and antibiotics (1% penicillin and streptomycin sulfate) at 37˚C in a humidified atmosphere of 5% CO_2. Medium containing NIH3T3 fibroblasts in the lower chamber served as a chemoattractant. The cells were then exposed to NO donor (GSNO 200 μM) and MEK inhibitor (U0126 10 μM). The chambers were incubated for 24 h, to determine invasion efficiency. HCT-116 cells were initially seeded on a 24-well plate at a density of $1x10^5$ cells/well and cultured in RPMI-1640/10% FBS, in the presence of 1% glutamine and antibiotics (1% penicillin and streptomycin sulfate) at 37˚C in a humidified atmosphere of 5% CO_2. Medium containing NIH3T3 fibroblasts in the lower chamber served as a chemoattractant. The cells were then exposed to NO donor (GSNO 200 μM) and MEK inhibitor (U0126 10 μM). The chambers were incubated for 48 h, to determine invasion efficiency. MIAPaCa-2 and HCT-116 cells on the upper surface of the filter were removed using a cotton-wool swab, and the cells that had invaded the lower surface were stained with 1% toluidine blue after fixation in 100% methanol. The number of invading cells was counted in 5 randomly selected fields under a light microscope. Each experiment was performed in triplicate.

Statistical analysis. Statistical analysis was performed using the StatView J-5.0 program (Abacus Concepts Inc., Berkeley, CA). Comparisons were carried out using Student's t-test, and $P<0.05$ were considered statistically significant. ANOVA followed by Tukey-Kramer post hoc test was used to compare multiple samples, with a significance level of 0.05.

Results

NO donor and MEK inhibitor influence IGF-I signaling in MIAPaCa-2 cells. Stimulation of IGF-I resulted in marked phosphorylation of IGF-IR, Akt and ERK1/2 in MIAPaCa-2 cells. GSNO, a NO donor, inhibited IGF-I-stimulated phosphorylation of IGF-IR and Akt. On the other hand, GSNO induced phosphorylation of ERK1/2 without stimulation of IGF-I, and enhanced IGF-1-stimulated phosphorylation of ERK1/2. However, GSNO did not influence IGF-IR, Akt, and ERK1/2 protein expression in MIAPaCa-2 cells. U0126, a MEK inhibitor, inhibited IGF-I-stimulated phosphorylation of ERK1/2. On the other hand, surprisingly, U0126 enhanced IGF-I-stimulated tyrosine phosphorylation of IGF-IR, without the influence of IGF-IR protein expression. In addition, U0126 upregulates IGF-I-stimulated phosphorylation of Akt. The combination of GSNO and MEK inhibitor inhibited IGF-I-stimulated phosphorylation of IGF-IR, Akt, and ERK1/2 without the influence of IGF-IR, Akt, and ERK1/2 protein expression (Fig. 1).

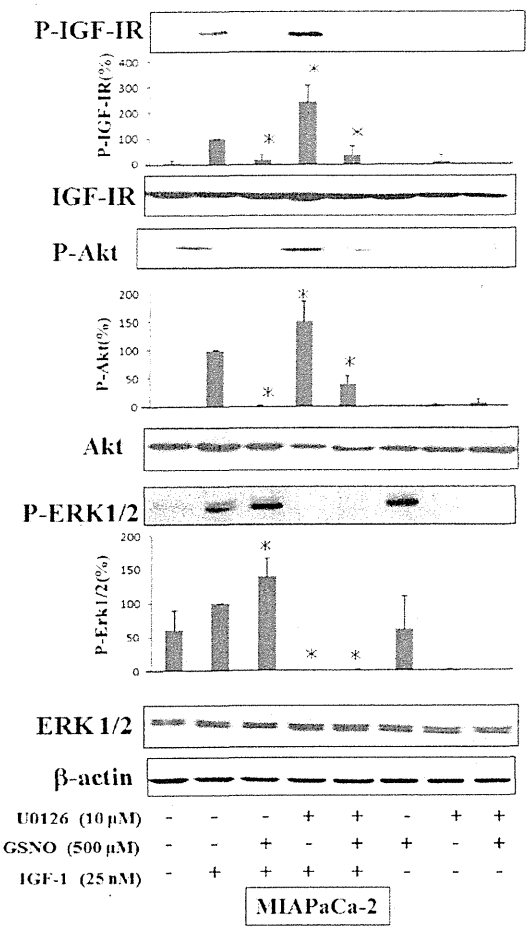

Figure 1. Regulation of insulin-like growth factor (IGF) signaling by nitric oxide (NO) donor and MEK inhibitor in MIAPaCa-2 cells. MIAPaCa-2 cells were incubated in DMEM with 10% FBS overnight and grown to 80% confluency. The cells were then incubated with S-nitrosoglutathione (GSNO) (500 μM) and U0126 (10 μM) for 6 h. After the starvation of serum for 2 h, the cells were incubated with IGF-I (25 nM) for 5 min and then harvested. Cell lysates were subjected to immunoblotting (IB). All experiments were repeated three times and similar results were obtained. Bands of interest were scanned by using Colorio GT-X970 and were quantified by using NIH Image 1.62 software. The results of densitrometry analysis of each band were compared to control, which was the band of IGF-I-stimulated p-Akt, p-ERK1/2, and p-IGF-IR without the administration of either GSNO or U0126. Error bars indicate the standard errors of the means. *P<0.05 compared to control.

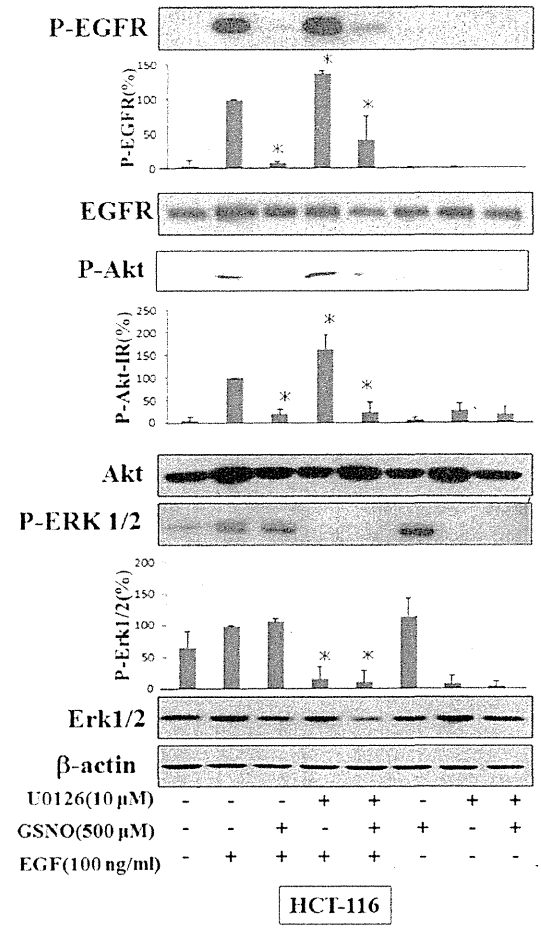

Figure 2. Regulation of EGF signaling by NO donor and MEK inhibitor in HCT-116 cells. HCT-116 cells were incubated in RPMI-1640 with 10% FBS overnight and grown to 80% confluency. The cells were then incubated with GSNO (500 μM) and U0126 (10 μM) for 6 h. After the starvation of serum for 2 h, the cells were incubated with EGF (100 ng/ml) for 5 min and then harvested. Cell lysates were subjected to immunoblotting. All experiments were repeated three times and similar results were obtained. Bands of interest were scanned by using Colorio GT-X970 and were quantified with NIH Image 1.62 software. The results of densitrometry analysis of each band were compared to control, which was the band of EGF-stimulated p-Akt, p-ERK1/2, and p-IGF-IR without the administration of either GSNO or U0126. Error bars indicate the standard errors of the means. *P<0.05, compared to control.

NO donor and MEK inhibitor influence EGF signaling in HCT-116 cells. Stimulation of EGF resulted in marked tyrosine phosphorylation of EGFR, Akt and ERK1/2 in HCT-116 cells. GSNO inhibited EGF-stimulated phosphorylation of EGFR and Akt. However, GSNO induced phosphorylation of ERK1/2 without stimulation of EGF, and enhanced EGF-stimulated phosphorylation of ERK1/2. U0126 inhibited EGF-stimulated phosphorylation of ERK1/2. On the other hand, surprisingly, U0126 enhanced EGF-stimulated tyrosine phosphorylation of EGFR without the influence of EGFR protein expression. In addition, U0126 upregulates EGF-stimulated phosphorylation of Akt. The combination of GSNO and U0126 inhibited EGF-stimulated phosphorylation of EGFR, Akt and ERK1/2 without the influence of EGFR, Akt, and ERK1/2 protein expression (Fig. 2).

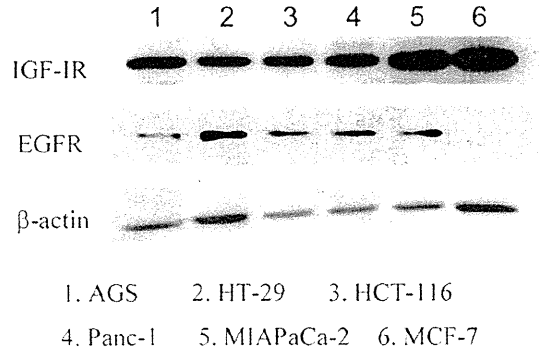

Figure 3. IGF-IR and EGFR protein expression in cancer cells. Cell lysates of MIAPaCa-2 cells, HCT-116, Panc-1, MCF-7, HT-29 and AGS cells were subjected to immunoblotting and then IGF-IR and EGFR protein was detected.

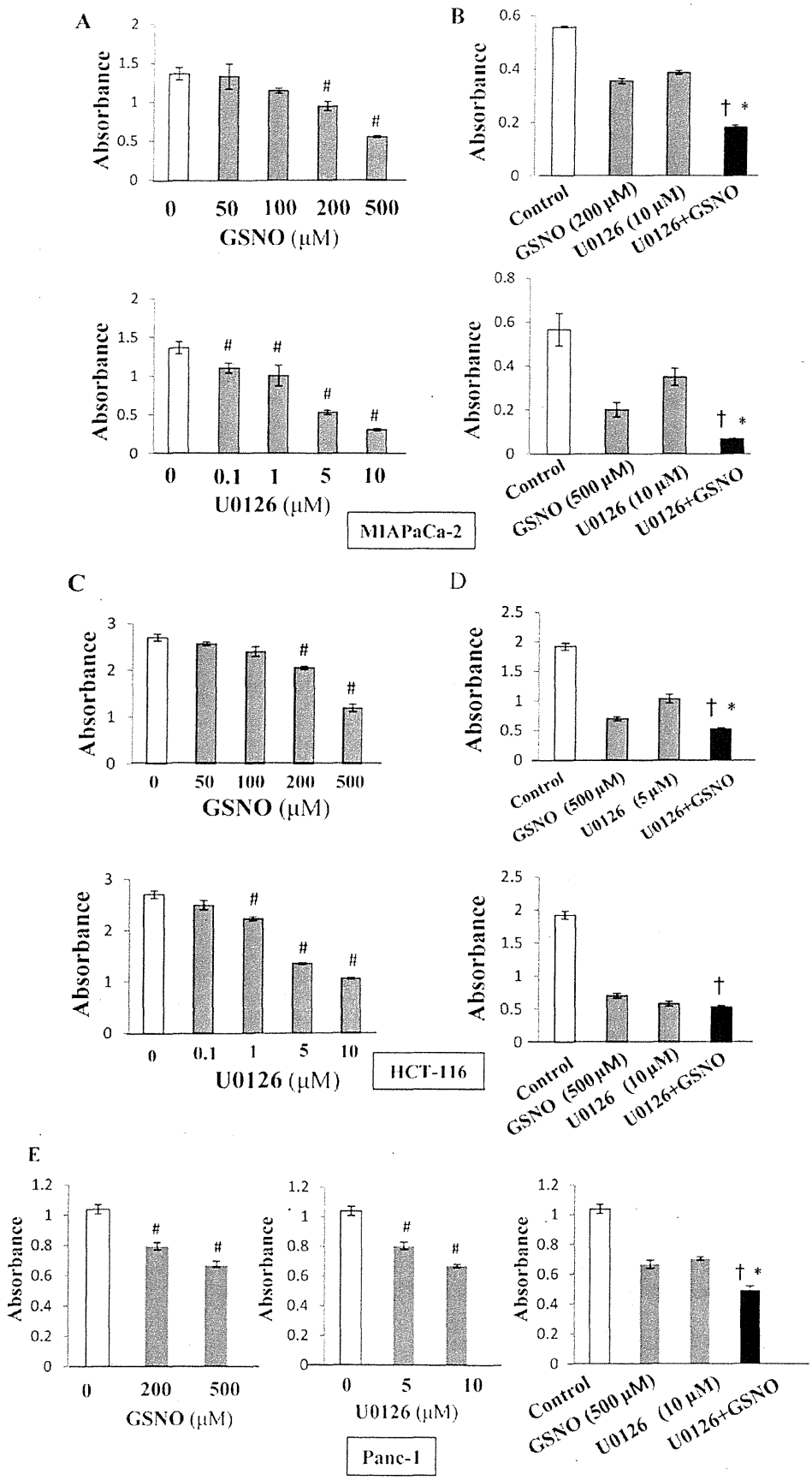

Figure 4. NO donor alone and MEK inhibitor alone significantly inhibit the proliferation of cancer cells in a dose-dependent manner, when the cells were incubated in medium containing with FBS. The combination of NO donor and MEK inhibitor inhibit the proliferation of MIAPaCa-2 cells compared to either NO donor or MEK inhibitor alone.